Dispersion analysis of an average-derivative optimal scheme for Laplace-domain scalar wave equation

Jing-Bo Chen[1]

ABSTRACT

Laplace-domain modeling is an important foundation of Laplace-domain full-waveform inversion. However, dispersion analysis for Laplace-domain numerical schemes has not been completely established. This hampers the construction and optimization of Laplace-domain modeling schemes. By defining a pseudowavelength as a scaled skin depth, I establish a method for Laplace-domain numerical dispersion analysis that is parallel to its frequency-domain counterpart. This method is then applied to an average-derivative nine-point scheme for Laplace-domain scalar wave equation. Within the relative error of 1%, the Laplace-domain average-derivative optimal scheme requires four grid points per smallest pseudowavelength, whereas the classic five-point scheme requires 13 grid points per smallest pseudowavelength for general directional sampling intervals. The average-derivative optimal scheme is more accurate than the classic five-point scheme for the same sampling intervals. By using much smaller sampling intervals, the classic five-point scheme can approach the accuracy of the average-derivative optimal scheme, but the corresponding cost is much higher in terms of storage requirement and computational time.

INTRODUCTION

Based on seismic data lacking low-frequency information, Laplace-domain full-waveform inversion (FWI) can yield a smooth velocity model that can be used as a starting model for subsequent frequency-domain FWI. Therefore, Laplace-domain FWI plays an important role in facilitating application of FWI to real data (Shin and Cha, 2008). The success of Laplace-domain FWI lies in that (1) the objective function in Laplace domain is much smoother than its frequency-domain counterpart, thus considerably mitigating the problem of local minima (Shin and Ha, 2008); (2) Lapace-domain FWI is less sensitive to the lack of low-frequency information in real seismic data in comparison with Fourier-domain FWI (Ha and Shin, 2012). Combined with conventional FWI, Lapace-domain FWI has made important contributions to the successful application of FWI to real data (Shin and Cha, 2009; Shin et al., 2010; Ha et al., 2012).

The key computational kernel of Laplace-domain FWI is Laplace-domain forward modeling. Numerical modeling schemes for frequency-domain modeling can be directly adapted to that for Laplace-domain modeling. However, the dispersion analysis of the Laplace-domain schemes has not been completely established (Shin and Cha, 2008). Shin et al. (2002) have developed a method to perform Laplace-domain numerical dispersion analysis. They express Laplace-domain dispersion relation as the square root of the ratio of numerical eigenvalue to analytical eigenvalue. However, this dispersion relation depends on damping constant, velocity, and sampling interval as well as propagation angle. Therefore, it is difficult to draw a general conclusion and to optimize the scheme.

To establish a more general method for Laplace-domain dispersion analysis, I will now examine the frequency-domain dispersion analysis. In frequency domain, the dispersion relation is expressed as the normalized phase velocity. This dispersion relation depends only on the number of grid points per wavelength as well as propagation angle. Therefore, the key is how to define a pseudowavelength in Laplace-domain. This pseudowavelength should be parallel to its frequency-domain counterpart. The concept of pseudowavelength is proposed in Shin et al. (2002) but its definition is not explicitly given.

Based on the skin depth in Laplace-domain acoustic wave equation (Um et al., 2012), a pseudowavelength in Laplace-domain can be defined as a scaled skin depth. Accordingly, a dispersion relation can be expressed as a normalized attenuation propagation velocity. In this way, just like the frequency-domain case, this dispersion relation depends only on the number of grid points per pseudowavelength as well as propagation angle. Therefore, on one hand, one

---

can easily draw a general conclusion on Laplace-domain dispersion analysis. For example, by performing dispersion analysis based on the normalized attenuation propagation velocity, one can draw a general conclusion that the classic five-point scheme in Laplace domain requires 13 grid points per smallest pseudowavelength to be within the relative error of 1%. On the other hand, one can perform optimization of Laplace-domain modeling schemes in the same way as in the frequency-domain case. Therefore, the frequency-domain average-derivative optimal scheme (Chen, 2012) can be easily adapted to the Laplace-domain case by performing the corresponding dispersion analysis and optimization.

In the next section, I will present the Laplace-domain average-derivative optimal scheme. This is followed by the optimization of coefficients and a numerical dispersion analysis. Numerical examples are then presented to demonstrate the theoretical analysis.

A LAPLACE-DOMAIN AVERAGE-DERIVATIVE SCHEME

Consider the 2D scalar wave equation in Laplace domain (Shin et al., 2002)

$$\frac{\partial^2 P}{\partial x^2} + \frac{\partial^2 P}{\partial z^2} - \frac{s^2}{v^2} P = 0, \tag{1}$$

where P is the pressure wavefield, the real number s is the Laplace damping constant, and $v(x, z)$ is the velocity. Numerical schemes for equation 1 can be directly obtained from the corresponding frequency-domain schemes. Frequency-domain schemes include the classic five-point scheme (Pratt and Worthington, 1990), the optimal nine-point scheme for equal directional sampling intervals (Jo et al., 1996), the average-derivative optimal scheme (Chen, 2012), and the directional-derivative optimal scheme (Chen, 2013).

Because the average-derivative optimal scheme accommodates general directional sampling intervals and has great flexibility in generalization (Chen, 2012), I apply the average-derivative method in this paper. Based on the frequency-domain scheme developed in Chen (2012), I consider an average-derivative nine-point scheme for equation 1

$$\frac{\bar{P}_{m+1,n} - 2\bar{P}_{m,n} + \bar{P}_{m-1,n}}{\Delta x^2} + \frac{\tilde{P}_{m,n+1} - 2\tilde{P}_{m,n} + \tilde{P}_{m,n-1}}{\Delta z^2}$$
$$- \frac{s^2}{v_{m,n}^2} [cP_{m,n} + d(P_{m+1,n} + P_{m-1,n} + P_{m,n+1} + P_{m,n-1})$$
$$+ b(P_{m+1,n+1} + P_{m-1,n+1} + P_{m+1,n-1} + P_{m-1,n-1})] = 0, \tag{2}$$

where

$$\bar{P}_{m+j,n} = \frac{1-\alpha}{2} P_{m+j,n+1} + \alpha P_{m+j,n} + \frac{1-\alpha}{2} P_{m+j,n-1},$$
$$j = 1, 0, -1, \tag{3}$$

$$\tilde{P}_{m,n+j} = \frac{1-\beta}{2} P_{m+1,n+j} + \beta P_{m,n+j} + \frac{1-\beta}{2} P_{m-1,n+j},$$
$$j = 1, 0, -1. \tag{4}$$

Here, $P_{m,n} \approx P(m\Delta x, n\Delta z)$, $v_{n,m} \approx v(m\Delta x, n\Delta z)$, Δx and Δz are sampling intervals in x- and z-directions, respectively, α, β, c, and d are weighted coefficients that should be optimized, and $b = \frac{1-c-4d}{4}$.

The average-derivative nine-point scheme (equation 2) includes the classic five-point scheme as a special case because when $\alpha = 1$, $\beta = 1$, $c = 1$, and $d = 0$, the scheme (equation 2) becomes

$$\frac{P_{m+1,n} - 2P_{m,n} + P_{m-1,n}}{\Delta x^2} + \frac{P_{m,n+1} - 2P_{m,n} + P_{m,n-1}}{\Delta z^2}$$
$$- \frac{s^2}{v_{m,n}^2} P_{m,n} = 0. \tag{5}$$

OPTIMIZATION AND DISPERSION ANALYSIS

Consider an attenuating function in the following form

$$P(k, r) = P_0 e^{-kr}, \tag{6}$$

where $r = \sin(\theta)x + \cos(\theta)z$, P_0 is the amplitude at $r = 0$, and θ is the propagation angle.

A skin depth δ is defined as the distance at which $P(k, r)$ is attenuated to $\frac{1}{e}$ of P_0 (Um et al., 2012). Therefore, $\delta = \frac{1}{k}$. A pseudowavelength λ is defined as the distance at which $P(k, r)$ is attenuated to $\frac{1}{e^{2\pi}}$ of P_0. According to this definition, $\lambda = \frac{2\pi}{k} = 2\pi\delta$ (Figure 1). Accordingly, k is defined as a pseudowavenumber. Substituting equation 6 into equation 1, one can obtain $\frac{s}{v} = k$. Thus, $v = \frac{s}{k} = \frac{s}{2\pi}\lambda$. In terms of this relation, v can be regarded as the propagation velocity of attenuation.

Substituting equation 6 into equation 2 and assuming a constant v, one obtains the discrete dispersion relation

$$\frac{s^2}{v^2} = \frac{A}{B\Delta x^2}, \tag{7}$$

where

$$A = \left[(1-\alpha)\cosh\left(\frac{2\pi\cos(\theta)}{RG}\right) + \alpha\right]\left[2\cosh\left(\frac{2\pi\sin(\theta)}{G}\right) - 2\right]$$
$$+ R^2\left[(1-\beta)\cosh\left(\frac{2\pi\sin(\theta)}{G}\right) + \beta\right]$$
$$\times \left[2\cosh\left(\frac{2\pi\cos(\theta)}{RG}\right) - 2\right],$$
$$B = c + 2d\left[\cosh\left(\frac{2\pi\cos(\theta)}{RG}\right) + \cosh\left(\frac{2\pi\sin(\theta)}{G}\right)\right]$$
$$+ 4b\cosh\left(\frac{2\pi\cos(\theta)}{RG}\right)\cosh\left(\frac{2\pi\sin(\theta)}{G}\right),$$

and where $G = \frac{2\pi}{k\Delta x}$ is the number of grid point per pseudowavelength, and $R = \frac{\Delta x}{\Delta z}$. Here, I consider the case $\Delta x \geq \Delta z$.

From equation 7, the numerical propagation velocity of attenuation can be derived as follows

$$V_{\text{num}} = \frac{s}{k} = \frac{v}{k\Delta x}\left(\frac{A}{B}\right)^{\frac{1}{2}}. \tag{8}$$

One can then obtain the normalized numerical propagation velocity of attenuation

$$\frac{V_{\text{num}}}{v} = \frac{G}{2\pi} \left(\frac{A}{B}\right)^{\frac{1}{2}}. \tag{9}$$

The coefficients α, β, c, and d are determined by minimizing the velocity error

$$E(\alpha, \beta, c, d) = \int \int \left[1 - \frac{V_{\text{num}}(\theta, \tilde{k}; \alpha, \beta, c, d)}{v}\right]^2 d\tilde{k}d\theta, \tag{10}$$

where $\tilde{k} = \frac{1}{G}$.

The ranges of $\tilde{k}$ and θ are taken as $[0, 0.25]$ and $[0, \frac{\pi}{2}]$, respectively. I use a constrained nonlinear optimization program fmincon in Matlab to determine the optimization coefficients. The optimization coefficients for different $R = \frac{\Delta x}{\Delta z}$ are listed in Table 1. The coefficients are different from their counterparts for frequency-domain average-derivative optimal scheme (Chen, 2012). This is because dispersion analysis in Laplace-domain is fundamentally different from that in Fourier-domain in spite of formal similarity between the two. In the same way, wavelength and pseudowavelength are two independent concepts although they share some formal similarity.

If $\Delta z > \Delta x$, one should define $G = \frac{2\pi}{k\Delta z}$, and $R = \frac{\Delta z}{\Delta x}$. For the case of $\Delta z > \Delta x$, the only change in the optimization coefficients is that the coefficients α and β are exchanged.

Now I perform numerical dispersion analysis. Figure 2 shows normalized numerical attenuation propagation velocity surfaces of the five-point scheme (equation 5) and the average-derivative optimal nine-point scheme (equation 2) for different propagation angles. The surface is a function of $\frac{1}{G}$ and $\frac{\Delta x}{\Delta z}$. For the five-point scheme (equation 5), the velocity errors increase with increasing $\frac{1}{G}$. On the other hand, the velocity errors decrease with increasing $\frac{\Delta x}{\Delta z}$ for $\theta = 0°$ and $\theta = 45°$ because of smaller Δz in comparison with Δx. For $\theta = 90°$, the velocity errors do not vary with $\frac{\Delta x}{\Delta z}$ because this case corresponds to horizontal propagation and has no relevance to Δz. For the average-derivative optimal nine-point scheme (equation 2), the velocity errors remain small for all values of $\frac{1}{G}$, $\frac{\Delta x}{\Delta z}$, and θ. Here, I only show the results for the case of $\Delta x \geq \Delta z$. For the case of $\Delta x < \Delta z$, similar results can be obtained.

Within the relative error of 1%, the five-point scheme (equation 11) requires 13 grid points per shortest pseudowavelength, whereas the average-derivative optimal nine-point scheme (equation 2) requires four grid points per shortest pseudowavelength for equal and unequal directional sampling intervals. For a heterogeneous media, the grid size is usually determined by using the minimum velocity. Another choice is to use the average velocity (Shin et al., 2002).

NUMERICAL EXAMPLES

In this section, I present numerical examples to verify the theoretical analysis on the average-derivative optimal nine-point scheme (equation 2) and the classic five-point scheme (equation 5).

Consider a homogeneous velocity model with a velocity of 2000 m/s. Horizontal and vertical distances are both 10 km (Figure 3). The Laplace damping constant s is taken to be 10π.

Accordingly, the pseudowavelength is $\lambda = 2000 \text{ m}/(10\pi/2\pi) = 400$ m. According to the criterion of four grid points per smallest pseudowavelength, horizontal sampling interval is determined by $\Delta x = 400 \text{ m}/4 = 100$ m. Vertical sampling interval is taken as $\Delta z = \Delta x/2 = 50$ m. For this ratio of directional sampling intervals, the optimization coefficients of the scheme (equation 2) are $\alpha = 0.828891$, $\beta = 0.866232$, $c = 0.693025$, and $d = 0.076743$ (Table 1). Horizontal and vertical samplings are $nx = 101$ and $nz = 201$, respectively. A Ricker wavelet with peak frequency of 5 Hz is placed at the center of the model as a source, and a receiver array is placed at a depth of 2.5 km.

For the analytical solution, the following formula is used (Alford et al., 1974)

$$P(x, z, s) = i\pi H_0^{(2)} \left(\frac{-is}{v} r\right) F(s), \tag{11}$$

where i is the imaginary unit, $H_0^{(2)}$ is the second Hankel function of order zero, $F(s)$ is the Laplace transform of the Ricker wavelet, and $r = \sqrt{(x - x_0)^2 + (z - z_0)^2}$. Here, (x_0, z_0) is the source position.
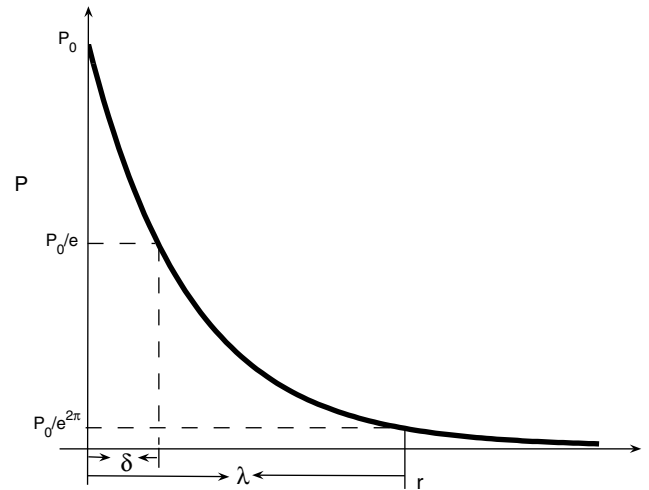

Figure 1. Schematic illustrating the concepts of skin depth and pseudowavelength. The vertical axis is the amplitude of the attenuation function in equation 6, and the horizontal axis represents the distance r.

Table 1. Optimization coefficients for α, β, c, and d for different $\frac{\Delta x}{\Delta z}$ when $\Delta x \geq \Delta z$.

	α	β	c	d
$\frac{\Delta x}{\Delta z} = 1$	0.863852	0.863852	0.693994	0.076501
$\frac{\Delta x}{\Delta z} = 1.5$	0.879003	0.851501	0.691999	0.077000
$\frac{\Delta x}{\Delta z} = 2$	0.828891	0.866232	0.693025	0.076743
$\frac{\Delta x}{\Delta z} = 2.5$	0.822773	0.862987	0.693373	0.076656
$\frac{\Delta x}{\Delta z} = 3$	0.834753	0.858629	0.693395	0.076651
$\frac{\Delta x}{\Delta z} = 3.5$	0.849042	0.855909	0.693397	0.076650
$\frac{\Delta x}{\Delta z} = 4$	0.860738	0.854423	0.693391	0.076652

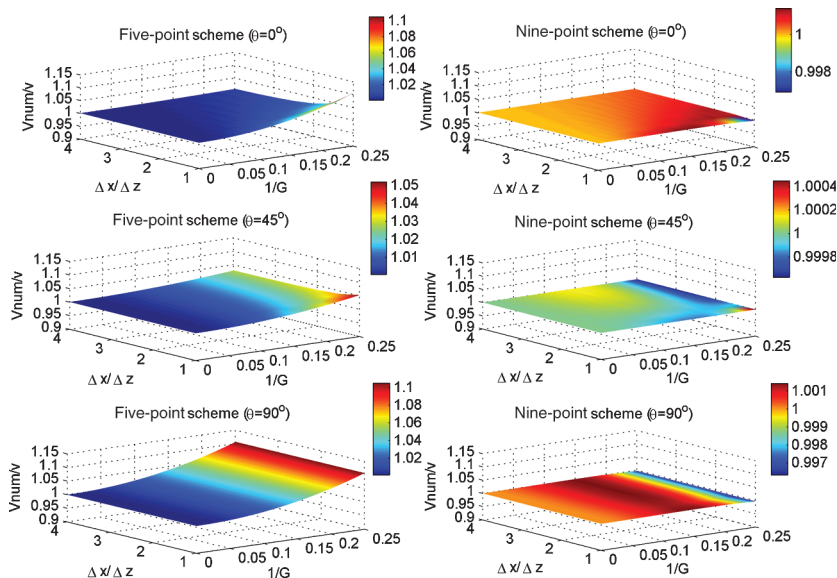In numerical comparisons, the following relative error of Laplace-domain wavefield is used

$$RE = \left| \frac{w_c - w_a}{w_a} \right|, \qquad (12)$$

where w_c and w_a are the calculated wavefield and the analytical wavefield, respectively.

Figure 4a shows the Laplace-domain seismograms computed with the analytical formula (equation 11), the classic five-point scheme (equation 5), and the average-derivative optimal nine-point scheme (equation 2). Figure 4b shows the corresponding relative errors of the classic five-point scheme (equation 5) and the average-derivative optimal nine-point scheme (equation 2). The five-point scheme and the nine-point scheme use the directional sampling intervals of $\Delta x = 100$ m and $\Delta z = 50$ m. The simulation result with the average-derivative optimal nine-point scheme (equation 2) is in good agreement with the analytical result. The result with the classic five-point scheme (equation 5) exhibits amplitude errors that become larger as the offset increases. The absolute errors shown in Figure 4a do not seem very large; however, the relative errors shown in Figure 4b are very large and reach 786% at far offsets. This is because of the extremely small values of the Laplace-domain wavefield at far offsets. Figure 4c is an enlarged part of Figure 4b, which zooms in on the relative errors of the average-derivative optimal nine-point scheme (equation 2). One can see that the relative error at far offsets is reduced to 21%.

In Figure 5, I show another case when the Laplace damping constant s is taken to be 5π. In this case, the five-point scheme (equation 5) and the average-derivative optimal nine-point scheme (equation 2) use the directional sampling intervals of $\Delta x = 200$ m and $\Delta z = 100$ m. Because of the smaller damping constant s, the wavefield is less attenuated in comparison with the case shown in Figure 4. Accordingly, the maximum relative error for the result computed with the five-point scheme (equation 5) becomes 170%, but it is still very large. For the average-derivative optimal nine-point scheme (equation 2), the relative error at far offsets is reduced to 15%.

The errors for the five-point scheme (equation 5) can be reduced by using smaller Δx and Δz, but this carries a much higher storage requirement and much longer computational time. Figure 6a shows the Laplace-domain seismograms computed with the analytical formula (equation 11), the classic five-point scheme (equation 5) with $\Delta x = 200$ m and $\Delta z = 100$ m, and the classic five-point scheme (equation 5) with $\Delta x = 62$ m and $\Delta z = 31$ m. Figure 6b shows the corresponding relative errors. One can see that the relative error at far offsets is reduced from 170% to 40% by using the smaller spacings. The Laplace damping constant s is taken to be 5π. From Figures 5 and 6, one can see that the result computed the classic five-point scheme (equation 5) with $\Delta x = 62$ m and $\Delta z = 31$ m approaches the accuracy of the average-derivative optimal nine-point scheme (equation 5) with $\Delta x = 200$ m and $\Delta z = 100$ m. However, for the classic five-point scheme (equation 2) with $\Delta x = 62$ m and $\Delta z = 31$ m, its storage requirement is approximately 32 times higher and its computational time is approximately seven times longer in comparison with that of the average-derivative optimal nine-point scheme (equation 2) with $\Delta x = 200$ m and $\Delta z = 100$ m.
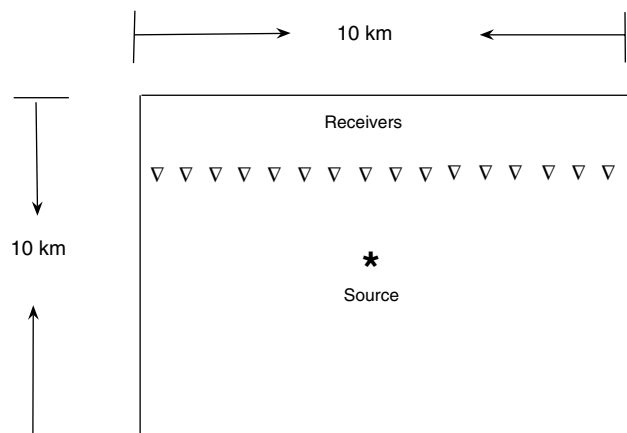

Figure 3. Schematic of the homogeneous model. A Ricker wavelet is placed at the center of the model as a source, and a receiver array is placed at a depth of 2.5 km.

Figure 2. Normalized numerical attenuation propagation velocity (V_{num}/v) surfaces of the five-point scheme (equation 5) and the average-derivative optimal nine-point scheme (equation 2) for different propagation angles. The surface is a function of $\frac{1}{G}$ and $\frac{\Delta x}{\Delta z}$.
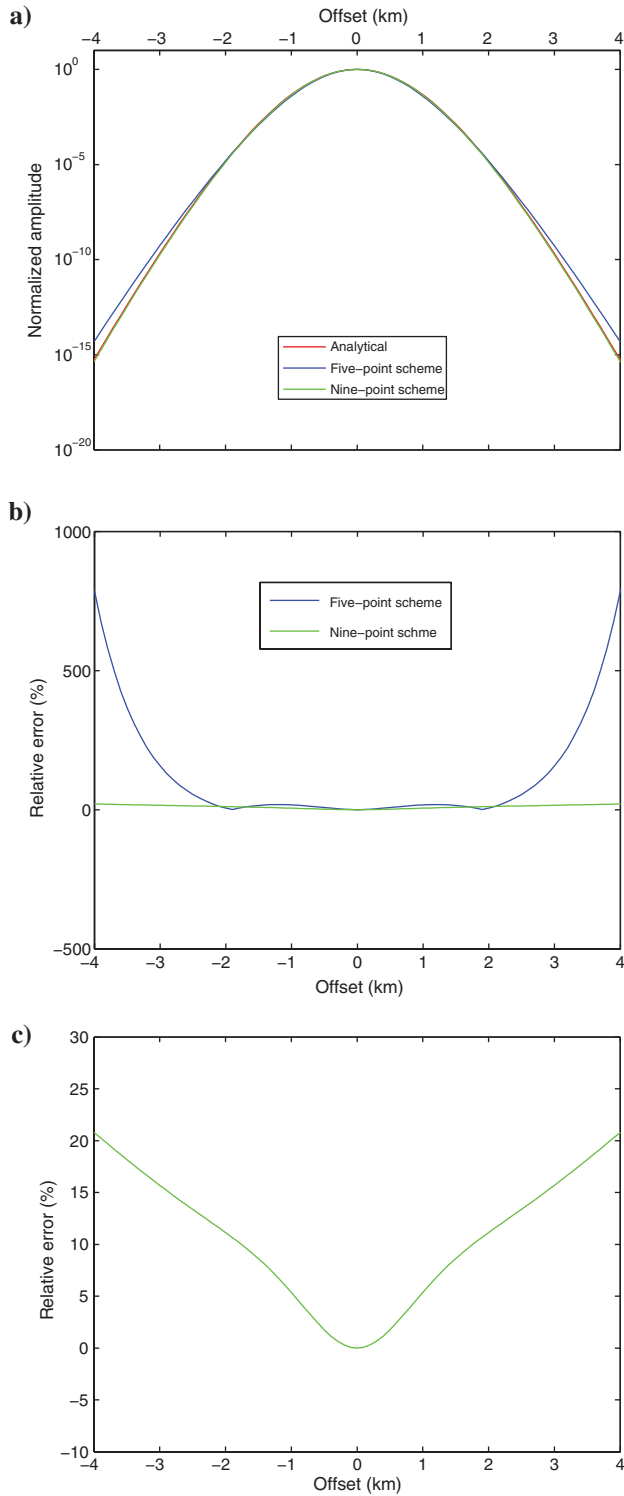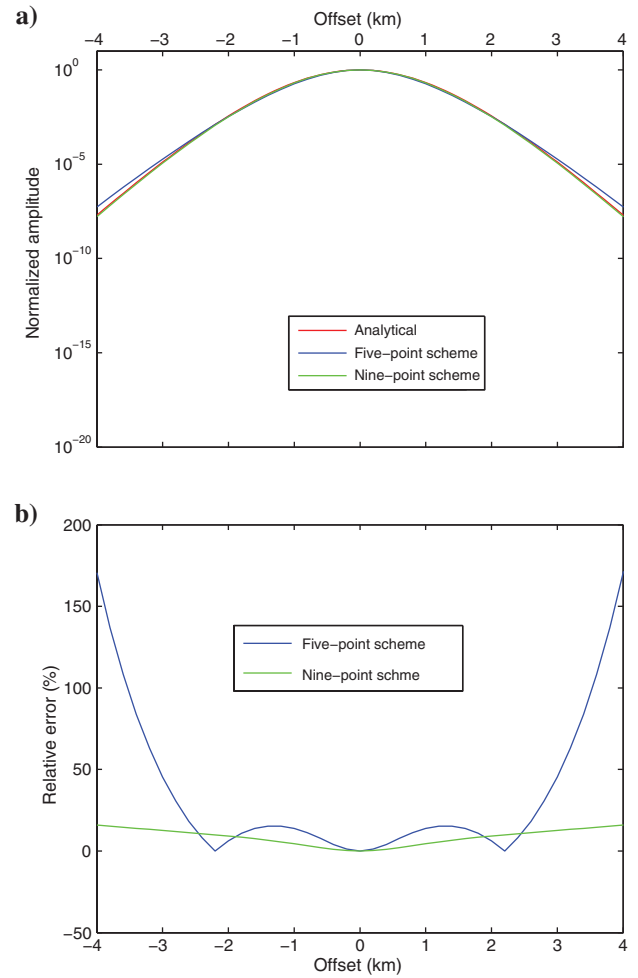
a)

b)

c)

Figure 4. Laplace-domain seismograms computed with the analytical formula (equation 11), the classic five-point scheme (equation 5), and the average-derivative optimal nine-point scheme (equation 2) (a), the corresponding relative errors (b), and an enlarged part of (b) in (c). The Laplace damping constant s is 10π, $\Delta x = 100$ m, and $\Delta z = 50$ m.

a)

b)

Figure 5. Laplace-domain seismograms computed with the analytical formula (equation 11), the classic five-point scheme (equation 5), and the average-derivative optimal nine-point scheme (equation 2) (a) and the corresponding relative errors (b). The Laplace damping constant s is 5π, $\Delta x = 200$ m, and $\Delta z = 100$ m.

CONCLUSIONS

By defining a pseudowavelength as 2π times the skin depth, I have developed a Laplace-domain method of numerical dispersion analysis. The resulting numerical attenuation propagation velocity depends on the pseudowavelength, which is parallel to its frequency-domain counterpart. Therefore, one can make use of the frequency-domain optimization technique. I have applied this Laplace-domain method of dispersion analysis to an average-derivative optimal nine-point scheme in Laplace domain. The resulting optimization coefficients are different from their frequency-domain counterparts. Compared to the classic five-point scheme, this Laplace-domain average-derivative optimal nine-point scheme reduces the number of grid points per shortest pseudowavelength from 13 to four for equal and unequal directional sampling intervals. Comparisons with the analytical solution for a homogeneous model demonstrate that the average-derivative optimal nine-point scheme is more accurate than the classic five-point scheme for the same sampling intervals, particularly at far offsets. The classic five-point scheme can approach the accuracy of the
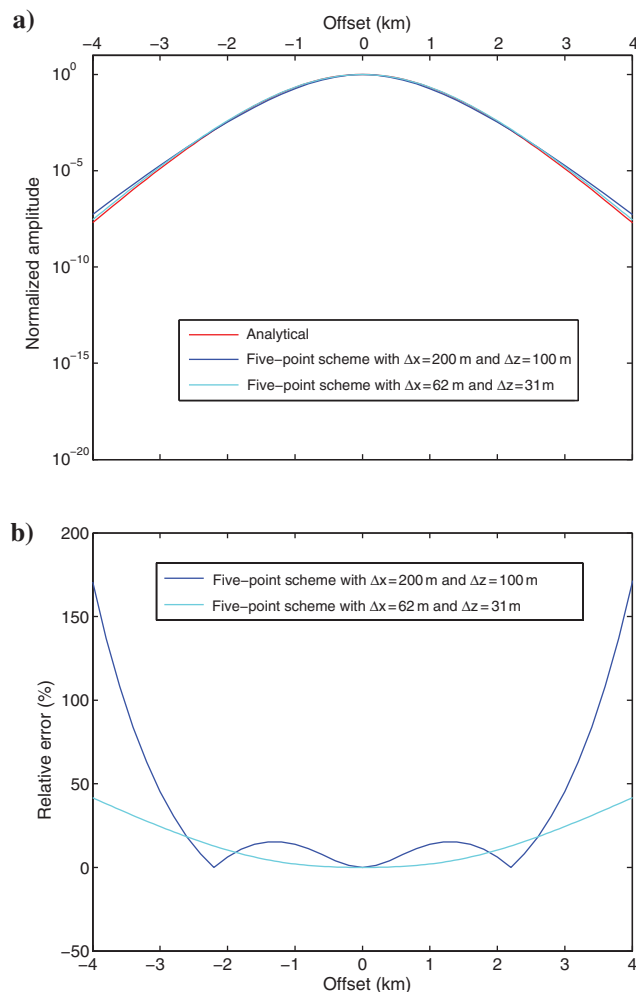
a)

b)

Figure 6. Laplace-domain seismograms computed with the analytical formula (equation 11), the classic five-point scheme (equation 5) with $\Delta x = 200$ m and $\Delta z = 100$ m, and the classic five-point scheme (equation 5) with $\Delta x = 62$ m and $\Delta z = 31$ m, (a) and the corresponding relative errors (b). The Laplace damping constant s is 5π.

average-derivative optimal nine-point scheme by using smaller spacings, but the corresponding storage requirement and computational time significantly increase.

ACKNOWLEDGMENTS

REFERENCES

Alford, R. M., K. R. Kelly, and D. M. Boore, 1974, Accuracy of finite-difference modeling of the acoustic wave equation: Geophysics, **39**, 834–842, doi: 10.1190/1.1440470.

Chen, J.-B., 2012, An average-derivative optimal scheme for frequency-domain scalar wave equation: Geophysics, **77**, no. 6, T201–T210, doi: 10.1190/geo2011-0389.1.

Chen, J.-B., 2013, A generalize optimal 9-point scheme for frequency-domain scalar wave equation: Journal of Applied Geophysics, **92**, 1–7.

Ha, W., W. Chung, E. Park, and C. Shin, 2012, 2-D acoustic Laplace-domain waveform inversion of marine field data: Geophysical Journal International, **190**, 421–428.

Ha, W., and C. Shin, 2012, Laplace-domain full-waveform inversion of seismic data lacking low-frequency information: Geophysics, **77**, no. 5, R199–R206, doi: 10.1190/geo2011-0411.1.

Jo, C.-H., C. Shin, and J. H. Suh, 1996, An optimal 9-point, finite-difference, frequency-space, 2-D scalar wave extrapolator: Geophysics, **61**, 529–537, doi: 10.1190/1.1443979.

Pratt, R. G., and M. H. Worthington, 1990, Inverse theory applied to multi-source cross-hole tomography, Part I: Scalar wave-equation method: Geophysical Prospecting, **38**, 287–310.

Shin, C., and Y. H. Cha, 2008, Waveform inversion in the Laplace domain: Geophysical Journal International, **173**, 922–931.

Shin, C., and Y. H. Cha, 2009, Waveform inversion in the Laplace-Fourier domain: Geophysical Journal International, **177**, 1067–1079.

Shin, C., and W. Ha, 2008, A comparison between the behavior of objective functions for waveform inversion in the frequency and Laplace domains: Geophysics, **73**, no. 5, VE119–VE133, doi: 10.1190/1.2953978.

Shin, C., N. H. Koo, Y. H. Cha, and K. P. Park, 2010, Sequentially ordered single-frequency 2-D acoustic waveform inversion in the Laplace-Fourier domain: Geophysical Journal International, **181**, 935–950.

Shin, C., D. J. Min, K. J. Marfurt, H. Y. Lim, D. Yang, Y. Cha, S. Ko, K. Yoon, T. Ha, and S. Hong, 2002, Traveltime and amplitude calculations using the damped wave solution: Geophysics, **67**, 1637–1647, doi: 10.1190/1.512811.

Um, E. S., M. Commer, and G. A. Newman, 2012, Iterative finite-difference solution analysis of acoustic wave equation in the Laplace-Fourier domain: Geophysics, **77**, no. 2, T29–T36, doi: 10.1190/geo2011-0220.1.